Accepted Manuscript

Geology, geochronology and isotopic geochemistry of the Xiaoliugou W-Mo ore field in the Qilian Orogen, NW China: Case study of a skarn system formed during continental collision

Yi Zheng, Xu Cai, Zhenju Ding, Peter A. Cawood, Suwei Yue

PII: S0169-1368(16)30037-3
DOI: doi: 10.1016/j.oregeorev.2016.01.013
Reference: OREGEO 1728

To appear in: *Ore Geology Reviews*

Received date: 20 June 2015
Revised date: 1 December 2015
Accepted date: 28 January 2016

Please cite this article as: Zheng, Yi, Cai, Xu, Ding, Zhenju, Cawood, Peter A., Yue, Suwei, Geology, geochronology and isotopic geochemistry of the Xiaoliugou W-Mo ore field in the Qilian Orogen, NW China: Case study of a skarn system formed during continental collision, *Ore Geology Reviews* (2016), doi: 10.1016/j.oregeorev.2016.01.013

Geology, geochronology and isotopic geochemistry of the Xiaoliugou W-Mo ore field in the Qilian Orogen, NW China: Case study of a skarn system formed during continental collision

Yi Zheng[a,b*], *Xu Cai*[a], *Zhenju Ding*[b], *Peter A. Cawood*[c,d], *SuweiYue*[e]

[a] *Guangdong Provincial Key Lab of Geological Processes and Mineral Resource Survey, Sun Yat-sen University, Guangzhou 510472, Guangdong, China*

[b] *Faculty of Earth Resources, China University of Geosciences, Wuhan 430074, Hubei, China*

[c] *Department of Earth Sciences, University of St. Andrews, North Street, St. Andrews KY16 9AL, UK*

[d] *School of Earth and Environment, University of Western Australia, WA 6009, Australia*

[e] *Guangzhou College, South China University of Technology, Guangzhou, 510800, Guangdong, China*

**Corresponding author: Yi Zheng*

Address: School of Earth Sciences and Geological Engineering, Sun Yat-sen University, Guangzhou 510275, China.

Tel.: +86 13929529874.

Email: zhengy43@mail.sysu.edu.cn (Y. Zheng)

Abstract

The Xiaoliugou W-Mo ore field lies within the mid-Paleozoic North Qilian Orogen, NW China, and hosts a W resource of 48.8 Mt @ 0.4% and 412.6 Mt of Mo @ 0.075%. It contains five deposits, including Xiaoliugou, Qiqing, Guishan, Qibao and Shiji. The main mineralization styles at Xiaoliugou are skarn and veins in which the mineral sequence is scheelite > molybdenite > chalcopyrite and occurs in the endo- and exo-contact zones of granite intrusions. The scheelite-dominated orebodies are overprinted by molybdenite-dominated quartz veins. Two molybdenite samples yielded Silurian Re-Os model ages of 427.4 ± 6.0 Ma and 428.2 ± 6.0 Ma. Three muscovite samples coexisting with molybdenite yielded Middle Devonian Ar-Ar ages of 392.0 ± 2.7 Ma, 391.1 ± 2.7 Ma and 391.4 ± 2.8 Ma. The Re-Os and Ar-Ar ages indicate that the W-Mo mineralization and alteration occurred at ca. 428–391 Ma, which corresponds with regional continental collision within the Qilian Orogen. $\delta^{34}S$ for the sulfides molybdenite and pyrite are 7.70–11.67 ‰ and 4.98–13.17 ‰, respectively. The $^{206}Pb/^{204}Pb$, $^{207}Pb/^{204}Pb$ and $^{208}Pb/^{204}Pb$ of the sulfides are 17.98–21.73, 15.34–18.81, and 37.18–38.63, respectively. The granites yield similar corrected $(^{206}Pb/^{204}Pb)_i$, $(^{207}Pb/^{204}Pb)_i$ and $(^{208}Pb/^{204}Pb)_i$, ranging 16.14–19.35, 15.44–15.63, and 37.41–38.31, respectively. Calculated $\delta^{18}O$ of the fluid inclusions in quartz range from -3.38–2.34 ‰, whereas the δD of the hydrothermal fluids ranges from -94 to -47 ‰. The S-, Pb-, O- and D-isotopic data imply that the metals originated from the granite intrusion with a minor component sourced from the host sediments, and that the ore-forming fluids were dominated by magmatic-hydrothermal fluids mixed with minor meteoric water.

Keywords: Xiaoliugou; Skarn; North Qilian Orogen; Geochronology; Isotope

geochemistry; Continental collision

1. Introduction

China's W and Mo reserves account for ca. 60% and 40% respectively, of the world's total resource (USGS, 2015). The majority of the W deposits are clustered in the Nanling region in South China (Fig.1A; Peng et al., 2006; Mao et al., 2013; Sheng et al., 2015), whereas the largest Mo ore field occurs within the Qinling and Dabie orogens in eastern-central China (Fig. 1A; Chen and Li, 2009; Chen et al., 2014; Huang et al., 2014. Wang et al., 2014; Li et al., 2015; Mi et al., 2015; Yang et al., 2015; Deng et al., in press). Recent exploration and research has shown that the North Qilian Orogen is a well-endowed W-Mo metallogenic province, with numerous large to small scale ore deposits, such as the Xiaoliugou W-Mo ore field that hosts the Xiaoliugou, Qiqing, Guishan, Qibao and Shiji deposits (Fig. 1B). The majority of these deposits were formed by magmatic-hydrothermal fluids associated with mid-Paleozoic granite intrusions, which are thought to have been emplaced in subduction- or continental collision settings (Mao et al., 1999; Yang et al., 2002; Xiao et al., 2003; Zhang et al., 2003; Zhou et al., 2004; Li, 2006; Jia et al., 2007; Zhang and Lin, 2010; Gao et al., 2011; Zhao et al., 2014). However, detailed investigation in the mineral assemblages is limited, and additional geochronological and geochemical research is needed to elucidate the mineralization processes and possible tectonic settings.

Among the deposits of the North Qilian Orogen, the Xiaoliugou W-Mo ore field is the largest, containing 48.76 Mt of W @ 0.4% and 412.63 Mt of Mo @ 0.075%, as well as exploitable Cu reserves (Fig. 2; 4th Geological Team of the Gansu Nonferrous Metals

Bureau, 2000). Published studies indicate that the mineralization occurs along the endo- and exo-contact zones of the porphyritic granite intrusions and within the related quartz veins (An and Zhou, 2002; Bai et al., 2005; Liu and Chen, 2005; Tang et al., 2006; Qiao, 2008).

In this study, we present a comprehensive analysis of mineral assemblages, molybdenite Re-Os and muscovite Ar-Ar geochronology and S-Pb-D-O isotope analyses within the Xiaoliugou W-Mo ore field. This data constrains the age of mineralization and alteration, the tectonic setting, and the source of metals and hydrothermal fluids enabling the development of a metallogenic model for the Xiaoliugou W-Mo ore field.

2. Regional Geology

The Xiaoliugou W-Mo ore field is located near the town of Qiqing (Sunan County) in Gansu, and is plcaed in the western part of the North Qilian Orogen (Feng and Wu, 1992; Zuo and Wu, 1997; Xia, 1998; Zuo et al., 2002; Du et al., 2004; Li, 2006; Xu et al., 2008). The North Qilian area is dominated by Precambrian and Paleozoic rocks (Fig. 1B; Li, 2006). The Lower Proterozoic Beidahe Group, Middle-Upper Proterozoic Jingtieshan Formation and the Upper Proterozoic Zhulongguan Formation are the main units hosting mineralization, and are unconformably overlain by a Paleozoic succession (Fig. 1B). The Precambrian rocks consist of schist, marble, biotite-amphibolite schist, and conglomerate intercalated with minor volcanic rocks. The Paleozoic lithostratigraphic sequences comprise Cambrian flysch, Middle Cambrian to Early Ordovician volcanic rocks intercalated with carbonate rocks, and upper Paleozoic sedimentary rocks (Li, 2006). Regional WNW-trending faults disrupt the rock units (Fig. 1B).

Granite intrusions in North Qilian account for less than 10% of the total area (Fig. 1B)

and are divided on the basis of age relationships into pre-, syn- and post- mid-Paleozoic tectono-thermal activity, which in China has traditional been referred to as Caledonian (e.g., Li et al., 2005). Zircon U–Pb dating results show that the syn-tectonic granites were emplaced between ca. 460 and 420 Ma (Mao et al., 2000; Wu et al., 2006;Jia et al., 2007; Zhang et al., 2008; Zhao et al., 2014). Wu et al. (2006) proposed that the granitic rocks older than ca. 440 Ma were formed in a subduction-related setting, whereas those younger than ca. 440 Ma were formed in a continental collision setting.

There are several W-Mo polymetallic deposits in the northwestern region of the North Qilian Orogen, including the Xiaoliugou W-Mo ore field, as well as the Ta'ergou W-Mo, Xiliugou W-Mo, Shidonggou Ag polymetallic deposits (Gao et al., 2011). The Xiliugou W-Mo and Shidonggou Ag polymetallic deposits are hosted in Precambrian rocks and are associated with the Yeniutan granitic pluton (zircon U–Pb ages: ca. 459–452 Ma; Mao et al., 2000), while the Xiaoliugou W-Mo deposit is genetically related to the Jinfosi granitic pluton (zircon U–Pb age: ca. 440 −420 Ma; Liu et al., 2009).

3. Local geology

The Xiaoliugou W-Mo ore field was first discovered in the mid-1990s by the 4th Geological Team of the Gansu Nonferrous Metals Bureau (4th Geological Team of the Gansu Nonferrous Metals Bureau, 2000). The ore field now consists of five single W-Mo-(Cu) deposits (Xiaoliugou, Qiqing, Guishan, Qibao and Shiji) (Figs. 2, 3A and 3B; Gao et al., 2011). The combined reserves of these deposits have been estimated to be 48.76 Mt at 0.4% W, 412.63 Mt at 0.075% Mo, and lesser concentrations of Cu, Be, Bi and Te (4th Geological Team of the Gansu Nonferrous Metals Bureau, 2000). Host rocks of the Xiaoliugou mine are the Precambrian Zhulongguan Group, which are composed of

marbles, phyllite, schists and siltstone subjected to greenschist–amphibolite facies metamorphism(Fig. 2).

Two sets of faults are recognized at the mine (Fig.2). One set trends WNW and constitutes part of the regional fault systemin the Qilian Orogen (Fig.2), whereas the other set occurs as radial faults in the exo-contact zone of the granite and controls the distribution of the orebodies (Fig.2).

Intrusions of monzogranite and granodiorite mainly lie south of the Xiaoliugou W-Mo mine area (Figs.3C and3D). Zhao et al (2014) reported a U-Pb zircon age for the monzogranite of 454.0 ± 2.0 Ma and for the granodiorite of 417.7 ± 1.7 Ma. The granodiorite is classified as S-type (ilmenite series) based on the ACF diagram (Mao et al., 1999).

Orebodies of the Xiaoliugou ore field generally occur as veins with lenticular shapes (Fig. 4). The scheelite-dominated orebodies are hosted in skarn along intrusive contacts (Figs. 4, 5A and 5B). In contrast, the molybdenite-dominated orebodies occur as fault-controlled steeply plunging lodes in the host rocks or scheelite-dominated orebodies (Fig. 5C). The scheelite-dominated orebodies appear to have been overprinted by the molybdenite-bearing quartz veins (Fig. 5D).

These two oretypes are classified as scheelite-skarn and molybdenite-quartz vein mineralization (Figs.5A, 5B and 5C).The skarn-type ores contain an average W grade of 0.67% and consist primarily of garnet, epidote, diopside, scheelite and fluorite with minor molybdenite (Figs. 5A and 5B), and the scheelite occurs as an interstitial phase of the above-mentioned skarn minerals. In contrast, the quartz veins contain muscovite, molybdenite, chalcopyrite, pyrrhotite, fluorite, wolframite and minor scheelite (Figs.5C,

5Dand 5E).

Detailed petrographic observations support a paragenetic sequence of early scheelite associated with garnet-epidote skarn, followed by molybdenite-bearing quartz veins. This is subsequently overprinted by pyrrhotite and chalcopyrite (Fig. 5). The interpreted paragenesis is evidenced by scheelite grains coated with later molybdenite (Fig. 5D), molybdenite-muscovite-quartz veins overprinted by chalcopyrite mineralization (Fig. 5E), and chalcopyrite coexisting and synchronous with the pyrrhotite (Fig. 5F).

4. Sampling and analytical methodology

4.1.Re-Os geochronology

Two molybdenite samples from Mo-bearing quartz veins, and containing the mineral assemblage molybdenite, quartz, muscovite and minor scheelite, were collected from diamond drill cores (Figs.4, 5C, 5D and5E). Samples were crushed to approximately 200 mesh and the molybdenite was separated by magnetic and gravitational methods, and then handpicked using a binocular microscope. Molybdenite Re-Os dating was completed at the Re-Os Laboratory of the National Research Center of Geoanalysis, Chinese Academy of Geological Sciences (CAGS). The analytical procedures are described in detail by Du et al. (2004), and the decay constant (λ) for ^{187}Re of1.666×10^{-11} year^{-1} was used (Smoliar et al., 1996).

4.2.Ar-Ar geochronology

Three muscovite samples were separated from the molybdenite-bearing quartz veins (Fig. 5C). Hand specimen and microscopic observation indicate the muscovite samples

are petrogenetically associated with the molybdenite-quartz veins and appear to be undeformed (Fig. 5C).

The samples were ultrasonically cleaned in distilled water, thenin acetone (three times each for 30 min) and then dried in preparation for irradiation. The samples and an international standard Brione muscovite (18.7 ± 0.09 Ma) (Hall et al., 1984) were wrapped in aluminum foil and stacked in quartz vials that were irradiated in the 49-2 reactor at the Beijing Atomic Energy Research Institute, with a flux of ~6.5×10^{12} cm^2 s^{-1} for 24 h, yielding J values of ~0.00646. Step-heating $^{40}Ar/^{39}Ar$ measurements were carried out at the Ar-Ar Laboratory of the Institute of Geology and Geophysics, Chinese Academy of Sciences (IGGCAS) in Beijing. Muscovite samples were incrementally heated from 800 to 1460 °C at a rateof 20 to 50 °C every 10 min. The isotopic measurement was made on a MM5400 mass spectrometer at IGGCAS. Detailed analytical procedures are described in Wang et al. (2006). The $^{40}Ar/^{39}Ar$ results were calculated and plotted using the ArCALC software (Koppers, 2002) and the decay constants of Steiger and Jager (1977). The age uncertainties are reported at the 95% confidence level (2σ). The plateau ages are defined according to the prerequisites introduced by Fleck et al. (1977). At least two steps with >80%of released ^{39}Arin total, whose ages are within 2σ of the mean value, were calculated by weighing with inverse variance.

4.3. S-Pb-D-O isotope analyses

Four sulfides and nine granite samples were analyzed for isotopes of S and Pb in this study. The sampling locations, occurrences and mineralogical compositions of sulfides

and granites are shown in Figures 3 and 4. Powders of pyrite, chalcopyrite and pyrrhotite finer than 200 mesh were mixed with copper oxide powder, and then heated to extract SO_2 gas. Sulfur isotope compositions of the extracted SO_2 were determined on a Finnigan Mat-251 mass spectrometer of the Analytical Laboratory of the Beijing Research Institute of Uranium Geology, China (CNNC). The $^{34}S/^{32}S$ ratios are expressed by the conventional $\delta^{34}S$ value in per mil relative to a Canon Diablo Troilite (CDT) standard, with an analytical precision of ±0.2 ‰. Lead isotopes analyses were conducted by first dissolving approximately 100mg of the sulfide powders in a $HF+HNO_3$ mixture. This was followed by drying and re-dissolution in 0.5 MHBr for Pb separation. A factor of 1% per mass unit for instrumental mass fractionation was applied to the Pb analyses using NBS 981 as a reference material. Measurements of the common Pb standard NBS 981 gave average values of $^{208}Pb/^{206}Pb = 2.1681 \pm 0.0008$, $^{207}Pb/^{206}Pb = 0.91464 \pm 0.00033$, $^{204}Pb/^{206}Pb = 0.059042 \pm 0.000037$, with uncertainties of < 0.1% at the 2σ level.

Ten representative quartz samples related to molybdenite or scheelite were selected for D-O isotopic analyses at CNNC, Beijing. The representative sample of quartz related to molybdenite is shown in Figure 5C, and the sampling location is marked in Figure 4. All the analyzed sulfide and quartz grains were separated through conventional preparation techniques including crushing, oscillation, heavy liquid and magnetic separation, followed by hand-picking under a microscope yielding concentrates with at least 99% purity. Oxygen isotope analyses were conducted on 10–30 mg of quartz finer than 200 mesh that was reacted with BrF_5 at 550–700 °C and converted to O_2. The purified $O_2$was reacted with a Pt-coated carbon rod at 700 °C to produce CO_2. The $^{18}O/^{16}O$ ratios are expressed by the conventional $\delta^{18}O$ value in per mil relative to the Pee Dee Belemnite

(PBD) standard, with an analytical precision of ±0.2‰. Approximately 5 g of 1–5 mm quartz grains were analyzed for H isotopes. The samples were first degassed of labile volatiles and then the secondary fluid inclusions were extracted by heating under vacuum to 120 °C for 3 h. The released water was trapped, reduced to H_2 by Zn, and then analyzed with a Finnigan Mat-251 mass spectrometer. The results of the analyses are expressed as δD with reported values relative to Standard Mean Ocean Water (SMOW), with an analytical precision of ± 2‰ (1σ).

5. Results

5.1. Age dating results

Results of the two molybdenite analyses in this studyand the published data of Mao et al. (1999) from the Xiaoliugou W-Mo ore field are listed in Table 1. The data range of Mao et al. (1999) is too large (496– 436 Ma), and therefore only the data analyzed in this study are summarized and discussed. The Re concentration in molybdenite measured in this study ranges from 6.22–14.87 ppm, and the ^{187}Os concentrations range 27.92–661.91 ppm. One sample has a model age of 427.4 ± 6.0 Ma, while the other yielded a model age of 428.2 ± 6.0 Ma (Table 1).The corresponding two ages of molybdenite confirm the Xiaoliugou deposit was formed at ca. 428 Ma.

The analytical results of step-heating ^{40}Ar/^{39}Ar measurements are listed in Table 2. The corresponding plateau ages and inverse isochron ages are plotted in Figure 6.The muscovite separates yielded plateau ages of 392.0 ± 2.7 Ma (MSWD = 0.03), 391.1 ± 2.7 Ma (MSWD=0.09) and 391.4 ± 2.8 Ma (MSWD=0.09), respectively, as defined by gas emissions from the 900–1300°C step-heating stages (with > 85% of ^{39}Ar gas released).

The inverse isochron age defined by total gas release of 12 stages is 392.2 ± 1.9 Ma (MSWD = 1.37), 391.1 ± 1.9 Ma (MSWD = 0.27) and 392.4 ± 2.4 Ma (MSWD = 1.73). The calculated initial $^{40}Ar/^{36}Ar$ values are 289.3 ± 7.3, 293.9 ± 6.6 and 278.5 ± 66.0, which coincide with the atmospheric value of 295.5 without Ar loss or addition (Kelley, 2002). In general, the normal and inverse isochron ages are consistent with the plateau ages, suggesting that the range of $^{40}Ar/^{36}Ar$ values is acceptable and the ages are geologically meaningful.

5.2. Sulfur isotopic compositions

Results of the S-isotope analyses for pyrite and molybdenite obtained in this study and data compiled from the literature are presented in Table 3. The $\delta^{34}S$ values for the molybdenite range 7.70−11.67‰, and pyrite range 4.98−13.17‰.

5.3. Lead isotopic compositions

The Pb isotope values for pyrite, molybdenite and chalcopyrite, granite and host rocks from this study combined with published data are presented in Table 4 and Figure 7. The sulfides from the Xiaoliugou deposit have $^{206}Pb/^{204}Pb$, $^{207}Pb/^{204}Pb$ and $^{208}Pb/^{204}Pb$ values of 17.98–21.73, 15.34–18.81 and 37.18–38.63, with average values of 18.66, 15.90 and 37.99, respectively. The granite yielded corrected $(^{206}Pb/^{204}Pb)_i$, $(^{207}Pb/^{204}Pb)_i$, and $(^{208}Pb/^{204}Pb)_i$ ratios with a range of 16.14–19.35 (mean = 17.78), 15.44–15.63(mean = 15.56), and 37.41–38.31 (mean = 37.95). In comparison, the host rocks have $^{206}Pb/^{204}Pb$, $^{207}Pb/^{204}Pb$, and $^{208}Pb/^{204}Pb$ ranging 18.15–18.46, 15.34–15.57, and 37.18–38.50, respectively.

5.4. D-O isotopic compositions

The D-O isotope analyses of quartz and fluid inclusions in quartz from the Xiaoliugou deposit are shown in Table 5 and Figure 8.The δD values of fluid inclusions in the mineralized quartz veins range from -94 to -47‰. The $\delta^{18}O$ values of vein quartz range from 9.5 to 16.3‰, with calculated $\delta^{18}O$ values of the fluids that formed the quartz ranging from -3.38 to 2.34‰. The D-O isotope diagram shows that the calculated hydrothermal fluid isotopic composition plots in the region between magmatic and meteoric water (Fig. 8).

6. Discussion

6.1.Source of metals and ore-forming fluids

Concentration of Re in molybdenite can be used to tracetheorigin of metals and tectonic settings due to a decrease of Re from the mantle to the crust(Mao et al., 1999; Stein et al., 2001a). Molybdenite sourced from mantle materials or oceanic crust shows higher Re concentrations ($n\times10^2$ppm), whereas molybdenite originating from continental crustal rocks contain lower Re concentrations (n– n×10 ppm; Stein et al., 2001b; Deng et al., 2014a, b; Mi et al., 2014). The molybdenite from the Xiaoliugou Mo deposit shows low Re contents (6.23–14.87 ppm) (Table 1), suggesting a crustal derivation.

The well-developed greisenization in the ores (Fig. 5C) implies that the ore-forming hydrothermal system had a pH<6 (Pirojno, 2009). Additionally, fluid inclusion homogenization temperatures were calculated to be below 500 °C (Zheng, 2008). This, combined with a lack of sulfate minerals associated with the ore, suggests that the sulfur

in the hydrothermal fluids system was mainly in the form of H_2S. Therefore, the sulfur of the sulfide represents the S-isotopic composition of hydrothermal fluids. The $\delta^{34}S$ values for the ore-forming fluids range from 4.98 to 13.17‰, which is significantly larger than that of magmatic sulfur (0±1‰) (Pirajno, 2009). The range of S-isotopic compositions is closer to that reported for sedimentary rocks (Leach et al., 2005; Gregory et al., 2015), which implies that there was a sedimentary source for the sulfur, possibly with a magmatic contribution.

Lead isotope compositions of pyrite, molybdenite, granite and host rocks are plotted in the diagram of Zartman and Doe(1981) (Fig. 7). The Pb-isotopic composition of pyrite is plotted between the upper crust and mantle fields and shows a steeply dipping distribution. This indicates the fluids that formed the pyrite were from a mixed source (Zartman and Doe, 1981). In contrast, the Pb-isotopic composition of molybdenite shows higher ^{206}Pb, U/Pb and Th/Pb, which coincide with the characteristics of high U and Th of the upper crust, indicating the fluids that formed the molybdenite originated from upper crustal sources (Zartman and Doe, 1981). Further comparison between the pyrite, molybdenite, granite and host rocks implies that the Pb composition of molybdenite is similar to the granite, and the Pb composition of pyrite is similar to the host rocks.

D-O isotopes can be used to trace the source of the mineralization fluids (e.g., Pirajno, 2009). The $\delta^{18}O$ andδD values for the ore-forming fluids at Xiaoliugouare plotted in the diagram of Taylor (1974) (Fig. 8). The quartz associated with scheelite and molybdenite yielded similar $\delta^{18}O$ and δD values,and plot between the magmatic and meteoric water fields, which implies that the scheelite and molybdenite originated from the same ore-forming fluid source. Considering the widespread granite distribution at Xiaoliugou

and in the North Qilian Orogen, we conclude that the ore-forming fluids at Xiaoliugou were mainly sourced from magmatic water with the involvement of minor meteoric water.

Previously studies showed that granite and host rocks in the region contain higher W and Mo concentrations than normal upper crustal rocks and granites(An and Zhou, 2002; Liu and Chen, 2005; Bai et al., 2005; Tang et al., 2006; Qiao, 2008). Combining this with our S-Pb-D-O isotope data, we conclude that the metals of Xiaoliugou W-Mo ore field were mainly derived from the granite intrusions but with a contribution of sedimentary rocks, and that the ore-forming fluids were dominated by magmatic-hydrothermal fluids mixed with minor meteoric fluids.

6.2.Ore-forming age and tectonic setting

Synthesis of the new molybdenite Re-Os and muscovite Ar-Ar ages show that the Xiaoliugou W-Mo mineralization occurred in range ca.430−390 Ma. The Ar-Ar ages are some 35−40 Ma younger than the Re-Os ages. This may have been due predominantly to systematic error, dating precision, or different closure temperatures of the two isotopic systems (Pirajno, 2009). Molybdenite has a closure temperature of ca. 500 °C (Stein et al., 2001b), whereas muscovite has a closure temperature of ca. 380 °C (Kelley, 2002). Granitic magma is estimated to take about 10 Ma to cool (Gao et al., 2011). Therefore, even a combination of systematic error, dating precision, and different closure temperatures are insufficient to account for the large age span, which may represent the time it took for the system to evolve from a skarn to vein-style mineralization.

The mineralization age of ca. 430−390 Ma is similar to the transition time from

crustal shortening to the post-orogenic extension within the North Qilian Orogen (Wu et al., 2006; Jia et al., 2007; Zhang et al., 2008). Geochemical discrimination diagrams of the intrusive rocks at Xiaoliugou also support a syn- to post-collision setting (Mao et al., 2000; Zhao et al., 2014). Combining with other geological and geochemical evidence, we conclude that the Xiaoliugou W-Mo deposit was formed in the Qaidam - North China collisional setting as illustrated in Figure 9. In addition, the start of mineralization at around 430 Ma post-dates regional models of the termination of subduction in the region (Wu et al., 2006). Similar long periods of mineralization have been identified in other continental collisional settings. The Yanshanian continental Mo metallogeny in Qinling occurred from ca. 156 to 109 Ma, with ore-forming events lasting ca.47 Ma (Li et al., 2011a, b, 2012a, b, c, 2013, 2014, 2015; Yang et al, 2012, 2013a, 2013b, 2014; Deng et al., 2013a,b,c, 2014a,b, 2015; Chen et al., 2014). The Au-Cu-Pb-Zn mineralization related to Indosinian collisional orogenesis in the Central Asian Orogenic Belt occurs from ca. 260–204 Ma (Zheng et al, 2012, 2013, 2015, 2016) over a period of 56 million years.

6.3.Implications for ore genesis

The skarn- and vein- type ores at Xiaoliugou are distributed along the intrusive contacts of associated granitic bodies (Figs. 2 and 3). The scheelite-dominated exo- and endo-skarn orebodies are overprinted by the molybdenite-rich quartz muscovite veins (Fig. 4). This suggests that the W in the Xiaoliugou deposit was formed as a typical skarn deposit and may have been later overprinted by Mo-bearing hydrothermal fluids.

Mao et al. (1999) showed that the granite and sedimentary host rocks contain higher W and Mo concentrations than usual. Additionally, our new Re-Os and S-Pb-D-O

isotopic data reveal that the metals of the ores originated from the granites with an additional contribution from the host sedimentary rocks.

Two molybdenite and three muscovite samples yielded alteration and mineralization ages of ca. 428–391 Ma, during the time in which the North Qilian Orogen was in transition from syn-orogenic crustal shortening to post-orogenic extension(Wu et al, 2006).

Based on the ore deposit geology, geochronology, and S-Pb-D-O isotope data of the Xiaoliugou W-Mo ore field, and in comparison with similar magmatic-hydrothermal deposits (i.e., Qinling and Dabie orogens, east-central China, Chen and Fu, 1992; Chen et al., 2004, 2005, 2008, 2009, 2014; Chen, 2006, 2013; Li et al., 2011a, b, 2012a, b, c, 2013, 2014, 2015; Yang et al, 2012, 2013a, 2013b, 2014; Deng et al., 2013a,b,c, 2014a,b, 2015; Liu et al., 2014, 2015; Wang et al., 2014; Mi et al., 2015), we conclude that the Xiaoliugou W-Mo ore field is a skarn W-Mo ore-forming system generated in a continental collision setting (Fig.9).

7. Conclusions

(1) Paragenetic sequence of the Xiaoliugou W-Mo mineralization is represented by early scheelite-bearing garnet-epidote skarn formation, followed by molybdenite-bearing quartz-muscovite vein mineralization, and overprinted by pyrrhotite and chalcopyrite.

(2) Molybdenite Re-Os and muscovite Ar-Ar dating constrains W-Mo mineralization to ca. 428-391 Ma, when the region was in a continental collision setting.

(3) Re-S-D-O-Pb isotope data imply that the metals originated from the granitic intrusion, with a contribution from the sedimentary host rocks, and that the ore-forming

fluids are dominated by magmatic-hydrothermal fluids with minor mixing with meteoric fluids.

Acknowledgements

This study is financially supported by the National Natural Science Foundation of China (41502068). Mr. Z-K Gao and D-FLiu of the 4th Geological Team of the Gansu Nonferrous Metals Bureau are thanked for providing field assistant. We also thank Profs. F. Pirajno and Y-J Chen, as well as Dr. X-H Deng and the two anonymous reviewers, whose comments and suggestions have greatly enhanced the paper.

References

4th Geological Team of the Gansu Nonferrous Metals Bureau, 2000. Prospecting Report of the Xiaoliugou W-Mo Deposit, Sunan, Gansu. Unpublished Document, Zhangye, pp 1–193(in Chinese).

An, T., Zhou, T.Q., 2002. The geological character and metallogenic model of W-multimetal ore deposit in Xiaoliugou, Gansu. Acta Geology Gansu 11, 54–66 (in Chinese with English abstract).

Bai, Z.W, Yang, Y., Mu, Z.F., 2005. Controlled factors and metallogenic relations of Xiaoliugou wolfram field in Gansu Provinces. Acta Geology Gansu 14, 64–69 (in Chinese with English abstract).

Chen, F., Qiao, L.B., Chen, J.P., 2007. Synthesis prospecting model in the Xiaoliugou W-Mo polymetallic mineralizing region, Gansu. Geology and Prospecting 43, 17–24 (in Chinese with English abstract).

Chen, Y.F., Z.W., Sun, C.P., 2010. Mineralization mechanism and exploration orientation of Xiaoliugou wolfram deposit in Gansu Province. Gansu Metall. 32, 75–80(in Chinese with English abstract).

Chen, Y.J., 2006. Orogenic-type deposits and their metallogenic model and explorationpotential. Geology in China 33, 1181–1196 (in Chinese with English abstract).

Chen, Y.J., 2013. The development of continental collision metallogeny and its application. Acta Petrol. Sin. 29, 1–17 (in Chinese with English abstract).

Chen, Y.J., Fu, S.G., 1992. Gold Mineralization in West Henan, China. China Seismological Press, Beijing, pp. 1–234 (in Chinese with English abstract).

Chen, Y.J., Pirajno, F., Sui, Y.H., 2004. Isotope geochemistry of the Tieluping silver deposit, Henan, China: a case study of orogenic silver deposits and related tectonic setting. Mineral. Deposita 39, 560–575.

Chen, Y.J., Pirajno, F., Qi, J.P., 2005. Origin of gold metallogeny and sources of ore-forming fluids, in the Jiaodong Province, eastern China. Int. Geol. Rev. 47, 530–549.

Chen, Y.J., Pirajno, F., Qi, J.P., 2008. The Shanggong gold deposit, eastern Qinling Orogen, China: isotope geochemistry and implications for ore genesis. J. Asian Earth Sci. 33, 252–266.

Chen, Y.J., Zhai, M.G., Jiang, S.Y., 2009. Significant achievements and open issues in study of orogenesis and metallogenesis surrounding the North China continent. Acta Petrol. Sin. 25, 2695–2726 (in Chinese with English abstract).

Chen, Y.J., Santosh, M., Somreville, I.D., Chen, H.Y., 2014. Indosinian tectonics and mineral systems in China: an introduction. Geol. J. 49, 331–337.

Chen, Y.J., Santosh, M., 2014. Triassic tectonics and mineral systems in Qinling Orogen, China. Geol. J. 49, 338–358.

Chen, Y.J., Li, N., 2009. Nature of ore-fluids of intracontinental intrusion-related hypothermal deposits and its difference from those in island arcs. Acta Petrol. Sin. 25, 2477–2508 (in Chinese with English abstract).

Deng, X.H., Chen, Y.J., Santosh, M., Yao, J.M., 2013a. Genesis of the 1.76 Ga Zhaiwa Mo – Cu and its link with the Xiong'er volcanics in the North China Craton: implications for accretionary growth along the margin of the Columbia supercontinent. Precambrian Res. 227, 337–348.

Deng, X.H., Chen, Y.J., Santosh, M., Yao, J.M., 2013c. Re-Os geochronology, fluid inclusions and genesis of the 0.85 Ga Tumen molybdenite–fluorite deposit in Eastern Qinling, China: implications for pre-Mesozoic Mo-enrichment and tectonic setting. Geol. J. 48, 484–497.

Deng, X.H., Chen, Y.J., Santosh, M., Zhao, G.C., Yao, J.M., 2013b. Metallogeny during continental outgrowth in the Columbia supercontinent: isotopic characterization of the Zhaiwa Mo–Cu system in the North China Craton. Ore Geol. Rev. 51, 43–56.

Deng, X.H., Chen, Y.J., Yao, L. J.M., Bagas,L., H.S. Tang. 2014a. Fluorite REE-Y (REY) geochemistry of the ca. 850 Ma Tumen molybdenitefluorite deposit, eastern Qinling, China: constraints on ore genesis. Ore Geol. Rev. 63, 532–543.

Deng, X.H., Santosh, M., Yao, J.M., Chen, Y.J., 2014b. Geology, fluid inclusions and sulfur isotope of the Zhifang Mo deposit in Qinling Orogen, central China: a case study of orogenic-type Mo deposits. Geol. J. 49, 515–533.

Deng, X.H., Chen, Y.J., Santosh, M., Yao, J.M., Sun, Y.L., in press. Re–Os and Sr–Nd–Pb isotope constraints on source of fluids in the Zhifang Mo deposit, Qinling Orogen,China. Gondwana Res., http://dx.doi.org/10.1016/j.gr.2015.02.020.

Dou, Y.J., 1999. Geology and origin of the Xiaoliugou scheelite deposit in Gansu. Geology exploration for Non-ferrous metals 8, 417–422 (in Chinese with English abstract) .

Du, A., Wu, S., Sun, D., Wang, S., Qu, W., Markey, R., Stein, H., Morgan, J., Malinovskiy, D.,2004. Preparation and certification of Re–Os dating reference materials: molybdenite HLP and JDC. Geostand. Geoanal. Res. 28, 41–52.

Du, Y.S., Zhu, J., Han, X., Hu, S.Z., 2004. From the back-arc basin to foreland basin: Ordovician-Devonian sedimentary basin and tectonic evolution in the North orogenic belt. Geol. Bull. China 23, 911–917 (in Chinese with English abstract).

Feng, Y.M., Wu, H.Q., 1992. Tectonic evolution of North Qilian Mountains and its neighborhood since Paleozoic. Northwest Geosci. 13, 61–74 (in Chinese with English abstract).

Fleck, R.J., Sutter, J.F., Elliot, D.H., 1977. Interpretation of discordant $^{40}Ar/^{39}Ar$ Age-Spectra of Mesozoic Tholeiites from Antarctica. Geochim.Cosmochim. Ac. 41, 15–32.

Gao, Z.K., Ding, Z.J., Song, S.G., Han, Y.Q., Chen, S.Y., 2011. Metallogenic system of tungsten-molybdenite associated with granite in Qilian orogenic belt. China University of Geosciences Press, Wuhan, China, pp.1–233(in Chinese with English abstract).

Gregory, D.D., Large, R.R., Halpin, J.A., Steadman, J.A., Hickman, A.H., Ireland, T.R., Holden, P., 2015. The chemical conditions of the late Archean Hamersley basin inferred from whole rock and pyrite geochemistry with $\Delta^{33}S$ and $\delta^{34}S$ isotope analyses. Geochim. Cosmochim. Act. 149, 223-250.

Hall, C.M., Walter, R.C., Westgate, J.A., York, D., 1984. Geochronology, stratigraphyand geochemistry of Cindery Tuff in Pliocene hominid-bearing sediments of the Middle Awash, Ethiopia. Nature 308, 26–31.

Huang, F., Wang, D.H., Wang, C.H., Chen, Z.H., Yuan, Z.X., Liu, X.X., 2014. Resources characteritics of Molybdenum deposit and their regional metallogeny in China. Acta Geol. Sin. 88, 2296-2314

Jia, Q.Z., Yang, Z.T., Xiao, Z.Y., 2007. Metallogenic regularity and prediction of Cu-Au-Pb-Zn deposits in Qilian Mountains. Geological publishing House, Beijing, pp 1–313(in Chinese with English abstract).

Kelley, S., 2002. K-Ar and Ar-Ar Dating. In: D. Porcelli, C.J. Ballentine and R. Wieler (Eds.). Noble Gases in Geochemistry and Cosmochemistry. Rev. Mineral Geochem.47, 785–818.

Koppers, A.A.P., 2002. ArArCALC-software for $^{40}Ar/^{39}Ar$ age calculations. Comput. Geosci. 28, 605–619.

Leach, D., Sangster, D., Kelley, K., Large, R. R., Garven, G., Allen, C., Gutzmer, J., and Walters, S., 2005, Sediment-hosted lead-zinc deposits: A global perspective. Economic Geology 100th, 561–607.

Li, N., Carranza, E.J.M., Ni, Z.Y., Guo, D.S., 2012c. The CO_2-rich magmatic – hydrothermal fluid of the Qiyugou breccia pipe, Henan Province, China: implication for breccia genesis and gold mineralization. Geochem. Explor. Environ. Anal., 12, 147–160.

Li, N., Chen, Y.J., Deng, X.H., Yao, J.M., 2014. Fluid inclusion geochemistry and ore genesis of the Longmendian Mo deposit in the East Qinling Orogen: implication for migmatitic-hydrothermal Mo-mineralization. Ore Geol. Rev. 63, 520–531.

Li, N., Chen, Y.J., Fletcher, I.R., Zeng, Q.T., 2011a. Triassic mineralization with Cretaceous overprint in the Dahu Au-Mo deposit, Xiaoqinling gold province: constraints from SHRIMP monazite U-Th-Pb geochronology. Gondwana Res. 20, 543–552.

Li, N., Chen, Y.J., Pirajno, F., Gong, H.J., Mao, S.D., Ni, Z.Y., 2012b. LA-ICP-MS zircon U-Pb dating, trace element and Hf isotope geochemistry of the Heyu granite batholith, eastern Qinling, central China: implications for Mesozoic tectono-magmatic evolution. Lithos, 142–143 , 34–47.

Li, N., Chen, Y.J., Pirajno, F., Ni, Z.Y., 2013. Timing of the Yuchiling giant porphyry Mo system, and implications for ore genesis. Mineral. Deposita 48, 505–524.

Li, N., Chen, Y.J., Santosh, M., Pirajno, F., 2015. Compositional polarity of Triassic granitoids in the Qinling Orogen, China: implication for termination of the northernmost paleo-Tethys. Gondwana Res. 27, 244–257.

Li, N., Chen, Y.J., Santosh, M., Yao, J.M., Sun, Y.L., Li, J., 2011b. The 1.85 Ga Mo mineralization in the Xiong'er Terrane, China: implications for metallogeny associated with assembly of the Columbia supercontinent. Precambrian Res. 186, 220–232.

Li, N., Ulrich, T., Chen, Y.J., Thomsen, T.B., Pease, V., Pirajno, F., 2012a. Fluid evolution of the Yuchiling porphyry Mo deposit, East Qinling, China. Ore Geol. Rev. 48, 442–459.

Li, W.Y., 2006. The metallogeny andexploration of the sulfide deposit in the North Qilian Mountains. Geological Press, Beijing, pp 1–207 (in Chinese with English abstract).

Liu, D.F., Chen, Y.F., 2005. Characteristics and mineralization appraise of quartz veins of Xiaoliugou wolfram deposit in Gansu Province. Contrib. Geol. Mineral Resour. Res. 20, 182–187 (in Chinese with English abstract).

Liu, J., Mao, J.W., Wu, G., Wang, F., Luo, D.F., Hu, Y.Q., Li, T.G., 2015.Fluid inclusions and H-O-S-Pb isotope systematics of the Chalukou giant porphyry Mo deposit, Heilongjiang Province, China. Ore Geol. Rev. 59, 83–96.

Liu, J., Mao, J.W., Wu, G., Wang, F., Luo, D.F., Hu, Y.Q., 2015. Geochemical signature of the granitoids in the Chalukou giant porphyryMo deposit in the Heilongjiang Province, NE China. Ore Geol. Rev. 64, 35–52.

Liu, X.H., Deng, J., Sun, B.N., Yan, F.Z., Ni, K.Q., Sun, X.L., Liu, J.F., Ni, S.G., 2009. Study on rock-forming and ore-forming of the Jinfosi pluton, western part of the North Qilian Mountains. Geological publishing house, Beijing, pp.1–128 (in Chinese with English abstract).

Mao, J.W., Zhang, Z.C., Zhang, Z.H., Du, A.D., 1999. Re-Os isotopic dating of molybdenites in the Xiaoliugou W (Mo) deposit in the northernQilian Mountains and its geological significance. Geochim. Cosmochim. Ac.63, 1815–1818.

Mao, J.W., Cheng, Y.B., Chen, M.H., Pirajno, P., 2013. Major types and time–space distribution of Mesozoic ore deposits in South China and their geodynamic settings. Mineral. Deposita 48, 267–294.

Mao, J.W., Zhang, Z.Z., Lehmann, B., Zhang, Z.C., Yang, J.M., Wang, Z.L., 2000. The Yeniutan granodiorite in Subei county, Gansu Province, China: Petrological features, geological settings and relationship to tungsten mineralization. Episodes 23, 163–171.

Mi, M., Chen, Y.J., Yang, Y.F., Wang, P., Li, F.L., Wan, S.Q., Xu, Y.L., 2015. Geochronology and geochemistry of the giant Qian'echong Mo deposit, Dabie Shan, eastern China: implications for ore genesis and tectonic setting. Gondwana Res. 27, 1217–1235.

Peng, J.T., Zhou, M.F., Hu, R.Z., 2006. Precise molybdenite Re–Os and mica Ar–Ar dating of the Mesozoic Yaogangxian tungsten deposit, central Nanling district, South China. Mineral. Deposita 41, 661–669.

Pirajno, F., 2009. Hydrothermal Processes and Mineral Systems. Springer, Berlin, pp. 1–1250.

Qiao, L.B. Zhang, Y.C, Lin, S., 2008. Gansu Qiqing Mo deposit quartz vein mineralization with relationship between Mo. Gansu Metall. 30, 32–35(in Chinese with English abstract).

Sheng, J.F., Chen, Z.H., Liu, L.J., Ying, L.J., Huang, F., Wang, D.H., Wang, J.H., Zeng, L., 2015. Outline of metallogeny of Tungsten deposits in China. Acta Geol. Sin. 89, 1038–1050

Smoliar, M.I., Walker, R.J., Morgan, J.W., 1996. Re–Os ages of group IIA, IIIA, IVA, and IVB iron meteorites. Science 271, 1099–1102.

Steiger, R.H., Jager, E., 1977. Subcommission on geochronology: Convention on the use of decay constants in geo- and cosmochronology. Earth Planet. Sci. Lett. 36(3), 359–362.

Stein, H.J., Markey, R.J., Morgan, J.W., Hannah, J.L., Schersten, A., 2001a. The remarkable Re–Os chronometer in molybdenite: how and why it works. Terra Nova 13, 479–486.

Stein, H.J., Markey, R.J., Morgan, J.W., Selby, D., Creaser, R.A., McCuaig, T.C., Behn, M., 2001b. Re–Os dating of Boddington molybdenite, SW Yilgarn: two Au mineralization events. AGSO-Geoscience Australia, Record 37, pp. 469–471.

Tang, J.R., Xi, X.S., Fan, X.R., An, T., Liu, D.F., 2006. Types and feature of the metallotectonic and Cu-W ore deposit mechanisms in Xiaoliugou, Gansu. Journal of Guilin Institute of technology 26, 174–180 (in Chinese with English abstract).

Taylor, H.P., 1974. The application of oxygen and hydrogen isotope studies to problems of hydrothermal alteration and ore deposition. Econ. Geol. 69, 843–883.

U.S. Geological Survey, 2015. Mineral commodity summaries 2015. U.S. Geological Survey, USA, pp. 1–198

Wang, F., Zhou, X.-H., Zhang, L.-C., Ying, J.-F., Zhang, Y.-T., Wu, F.-Y., Zhu, R.-X., 2006.Late Mesozoic volcanism in the Great Xing'an Range (NE China): timing and implications for the dynamic setting of NE Asia. Earth Planet. Sci. Lett.251, 179–198.

Wang, H.F, Zhou, J.Q., 2009. Xiaoliugou tungsten-molybdenum ore-mining features and explore the genesis of ore deposits, Gansu Metallurgy 31, 50–52 (in Chinese with English abstract).

Wang, P., Chen, Y.J., Fu, B., Yang, Y.F., Mi, M., Li Z.L., 2014. Fluid inclusion and H-O isotope geochemistry of the Yaochong porphyry Mo deposit in Dabie Shan, China: a case study of porphyry systems in continental collision orogenesis. Int. J. Earth Sci. 103, 777–797.

Wu, C.L., Yao, S.Z, Yang, J.S., Zeng, L.S., Chen, S.Y., Li, H.B., Qi, X.X., Wooden, J.L., Mazdab, F.K., 2006. Double-subduction of the Early Paleozoic North Qilian, NW China. Geology in China 53, 1197–1208 (in Chinese with English abstract).

Xia, L.Q., Xia, Z.C., Xu, X.Y., 1998. Early Paleozoic mid-ocean ridge-ocean island and back-arc basin volcanism in the North Qilian mountains. Acta Geol. Sin. 72, 301–312 (in Chinese with English abstract).

Xiao, Z.Y. Zou, X.H., Jia, Q.Z., Yang, Z.T., Xiao, S.Y., Duan, Y.M., Su, L.H., 2003. Present situation of the mineral resources in Qilian metallogenic belt and thinking. Northwestern Geology 36, 38–49 (in Chinese with English abstract).

Xu, X.Y., He, S.P., Wang, H.L., Chen, J.L., Zhang, E.P., Feng, Y.M., 1982. Geological survey for northwest of China. Beijing: Science Press, pp. 1–347 (in Chinese with English abstract).

Yang, Y., Chen, Y.J., Li, N., Mi, M., Xu, Y.L., Li, F.L., Wan, S.Q., 2013b. Fluid inclusion and isotope geochemistry of the Qian'echong giant porphyry Mo deposit, Dabie Shan, China: a case of NaCl-poor, CO2-rich fluid systems. J. Geochem. Explor. 24, 1–13.

Yang, Y., Chen, Y.J., Zhang, J., Zhang, C., 2013a. Ore geology, fluid inclusions and four-stage hydrothermal mineralization of the Shangfanggou giant Mo-Fe deposit in Eastern Qinling, central China. Ore Geol. Rev. 55, 146–161.

Yang, Y.F., Li, N., Chen, Y.J., 2012. Fluid inclusion study of the Nannihu giant porphyry Mo – W deposit, Henan Province, China: implications for the nature of porphyry ore-fluid systems formed in a continental collision setting. Ore Geol. Rev. 46, 83–94.

Yang, Y.F., Chen, Y.J., Pirajno, F., Li, N., 2015. Evolution of ore fluids in the Donggou giant porphyry Mo system, East Qinling, China, a new type of porphyry Mo deposit: Evidence from fluid inclusion and H-O isotope systematics. Ore Geol. Rev. 65, 148–164.

Yang, Z.T., Jia, Q.Z., Xiao, Z.Y., Zou, X.H., Ye, D.J., Duan, Y.M., Zhao, J.W., Su, L.H., 2002. Metallogenic geological conditions of Ta'ergou-Xiaoliugou W-collecting area and regional prospecting in Qilian metallogenic belt. Mineral Deposits 21, 515–518 (in Chinese with English abstract).

Zartman, R.E., Doe, B.R., 1981. Plumbotectonics- the model. Tectonophysics 75, 135–162.

Zhang, L.Y. Qu, X.M., Xin, H.B., 2008. Geochemical characteristics, zircon U-Pb LA-ICP-MS ages of medium-acid dykes in the Huashugou iron-copper deposit, Jingtieshan orefield and their geological significances. Geol. Rev. 54, 253–262 (in Chinese with English abstract).

Zhang, Z.S., Liu, S., 2010. Characteristics of REE geochemistry of the ore-bearing concealed granite in Xiaoliugou, Gansu Province. Journal of Henan polytechnic University (Natural Science) 29, 173–179 (in Chinese with English abstract).

Zhao, X.M., Zhang, Z.H., Liu, M., Li, Y.S., Guo, S.F., 2014. Zircon U-Pb geochronology, geochemistry and petrogenesis of the Xiaoliugou in the western of the North Qilian. Acta Petrol. Sin. 30, 16–34 (in Chinese with English abstract).

Zheng, Y., 2008. The study on geological characteristics and genesis of W-Mo deposit in Xiaoliugou. Bachelor thesis of China University of Geosciences (Wuhan). Unpublished, Wuhan, China, pp 1–38 (in Chinese with English abstract).

Zheng, Y., Zhang, L., Chen, Y.J., Pete, Hollings, Chen, H.Y., 2013. Metamorphosed Pb-Zn-(Ag) ores of the Keketale VMS deposit, Xinjiang: Evidence from ore textures, fluid inclusions, geochronology and pyrite compositions. Ore Geol. Rev. 54, 167–180.

Zheng, Y., Zhang, L., Chen, Y.J., Qin, Y.J. and Liu, C.F., 2012. Geology, fluid inclusion geochemistry, and $^{40}Ar/^{39}Ar$ geochronology of the Wulasigou Cu deposit, and their implications for ore genesis, Altay, Xinjiang, China. Ore Geol. Rev. 49, 128–140.

Zheng, Y., Zhang, L., Li, D.F., Argyrios, K., Chen, Y.J., 2015a. Genesis of the Dadonggou Pb–Zn deposit in Kelan basin, Altay, NW China: Constraints from zircon U–Pb and biotite $^{40}Ar/^{39}Ar$ geochronological data. Ore Geol. Rev. 64, 128–139.

Zheng, Y., Chen, Y.J., Cawood, P., Wang, Y.J., Chen, H.Y., Zhang, L., Li, D.F., 2016. Late Permian-Triassic metallogeny in the Chinese Altay Orogen: Constraints from mica $^{40}Ar/^{39}Ar$ dating on ore deposits. Gondwana Res. DOI: 10.1016/j.gr.2015.08.018.

Zhou, H., 2004. Ore fluid characteristics of Xiaoliugou tungsten deposit. Contributions to geology and mineral resources research 19, 110–113 (in Chinese with English abstract).

Zhou, T.G., Zhang, D.Z., Zhou, H., 1999. Geological features and genesis of the Xiaoliugou Cu-W polymetallic deposit in Gansu. Northwestern Geology 32, 1–10 (in Chinese with English abstract).

Zuo, G.C., Liu, Y.K., Zhang, C., 2002. Tectono-stratigraphic characteristics of continent crustal remnants in central-western sector of the North Qilian orogen. Scientia Geologica Sinica 37, 302–312 (in Chinese with English abstract).

Zuo, G.C., Wu, H.Q., 1997. A bi-subduction collision orogenic model of Early Paleozoic in the middle part of North Qilian area. Adv. Earth Sci. 12, 315–323 (in Chinese with English abstract).

Figure captions

Fig. 1. (A) Tectonic framework of China, showing the location of the North Qilian Orogen (modified after Chen et al., 2014); and distribution of main W and Mo deposits in China. (B)Tectonic framework of the North QilianOrogen (modified after Li et al., 2006).

Fig. 2. Geological map of the Xiaoliugou mineral district, including the Xiaoliugou, Qiqing, Shiji, Qibao W-Mo-(Cu) polymetallic deposits (modified after the 4th Geological Team of the Gansu Nonferrous Metals Bureau, 2000).

Fig. 3. Photographs and photomicrographs illustrating the Xiaoliugou mine and the granite related to mineralization. (A)Locations of the Xiaoliugou and Qibao deposits and their inland plateau geomorphology with strong denudation. (B)The W-Mo-bearing quartz veins at Xiaoliugou. (C)Altered granodiorite and monzogranite in drill cores. (D) Major minerals of monzogranite, including plagioclase, muscovite and quartz. Abbreviations: Ms=muscovite, Pl=plagioclase, Qtz=quartz.

Fig. 4.Cross section of the No.2 line at the Xiaoliugou W-Mo ore field (modified after the 4th Geological Team of the Gansu Nonferrous Metals Bureau, 2000).

Fig. 5. Photographs and photomicrographs showing the geological characteristics of the Xiaoliugou deposit. (A) Skarn-types ore containing pyrite, garnet and epidote; (B) Scheelite grows under ultraviolet light; (C) Quartz vein-type ore containing molybdenite and muscovite; (D) Molybdenite in quartz veins enveloping scheelite grain, implying molybdenite formed later than scheelite under the oblique light; (E) Chalcopyrite mineralization along the cleavage planes of molybdenite, implying molybdenite formed earlier than chalcopyrite under the reflected light; (F) Chalcopyrite coexists with pyrrhotite under the reflected light. Abbreviations: Py=pyrite, Grt=garnet, Ep=epidote, Mo=molybdenite, Ms=muscovite, Ccp=chalcopyrite, Po=pyrrhotite, Qtz=quartz.

Fig. 6. Muscovite $^{39}Ar/^{40}Ar$ stepwise laser ablation dating results

(A) Plateau age of sample PD30120-KZD-B2; (B) Normal isochron age of sample PD30120-KZD-B2; (C) Plateau age of sample PD30120-KZD-B5; (E) Normal isochron age of sample PD30120-KZD-B5; (C) Plateau age of sample PDQB-KZD-B4; (E) Normal isochron age of sample PDQB-KZD-B4.

Fig. 7.Lead isotopic compositions of sulfides, granite, and ore-hosting sediements for the Xiaoliugou W-Mo ore field.

Fig. 8.$\delta^{18}O$-δD plots for ore-forming fluids at Xiaoliugou. Compositions of meteoric-, magmatic- and metamorphic water from Taylor (1974)

Fig. 9. Tectonic-magmatic evolution model of the Xiaoliugou W-Mo deposit.

Table captions

Table 1.Molybdenite Re-Os dating results.

Table 2.Muscovite $^{39}Ar/^{40}Ar$ stepwise laser ablation dating results.

Table 3.Sulfur isotopic compositions of pyrite and molybdenite.

Table 4.Leadisotopic data of sulfides, granite and ore-hostingsediments.

Table 5.Quartz oxygen and hydrogen isotopic data.

Conflict of interest statement

We declare that we have no financial and personal relationships with other people or organizations that can inappropriately influence our work, there is no professional or other personal interest of any nature or kind in any product, service and/or company that could be construed as influencing the position presented in, or the review of, the manuscript entitled as "Geology, geochronology and isotopic geochemistry of the Xiaoliugou W-Mo skarn ore field in the Qilian Orogen, NW China: Case study of a skarn system during continental collision".

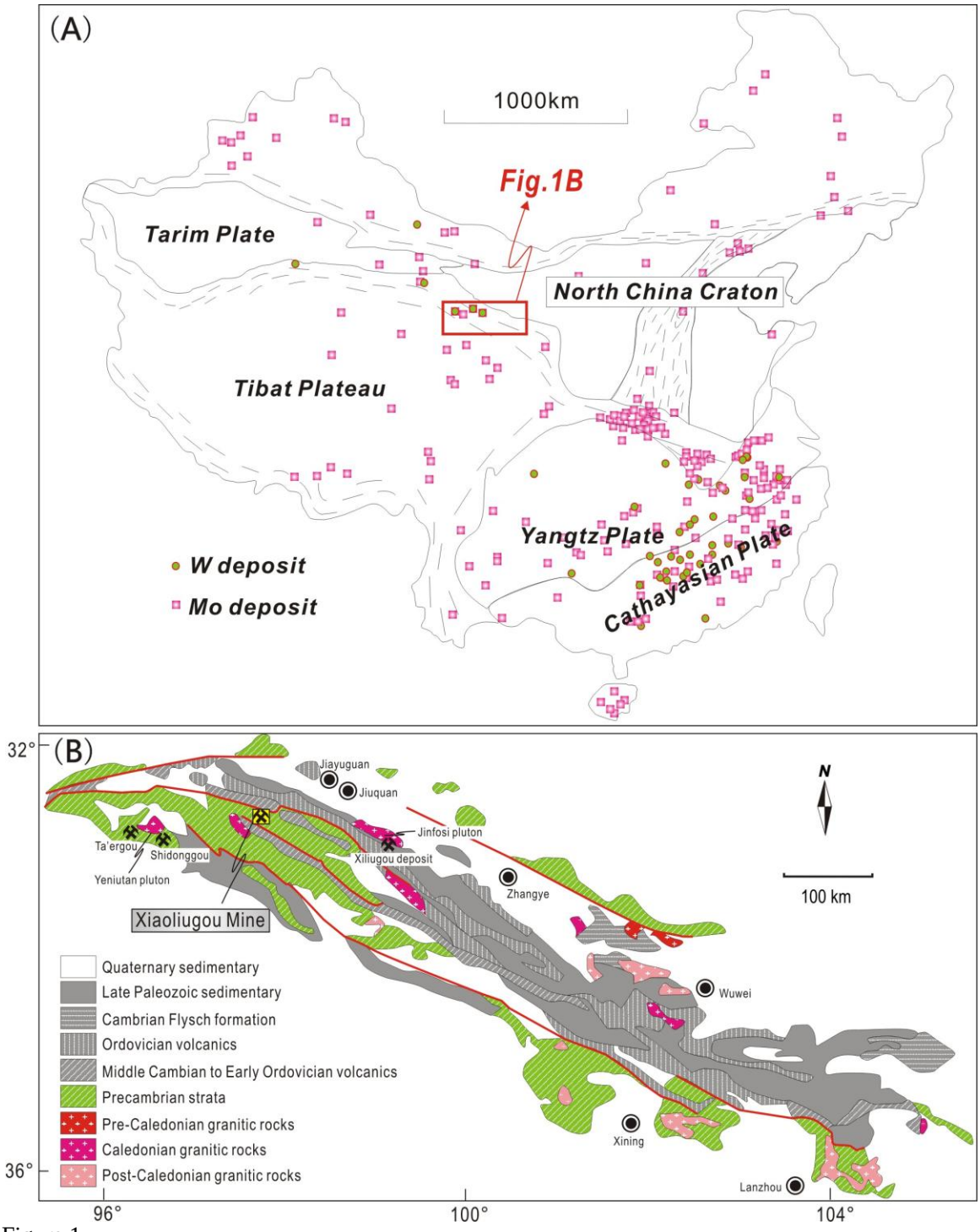

Figure 1

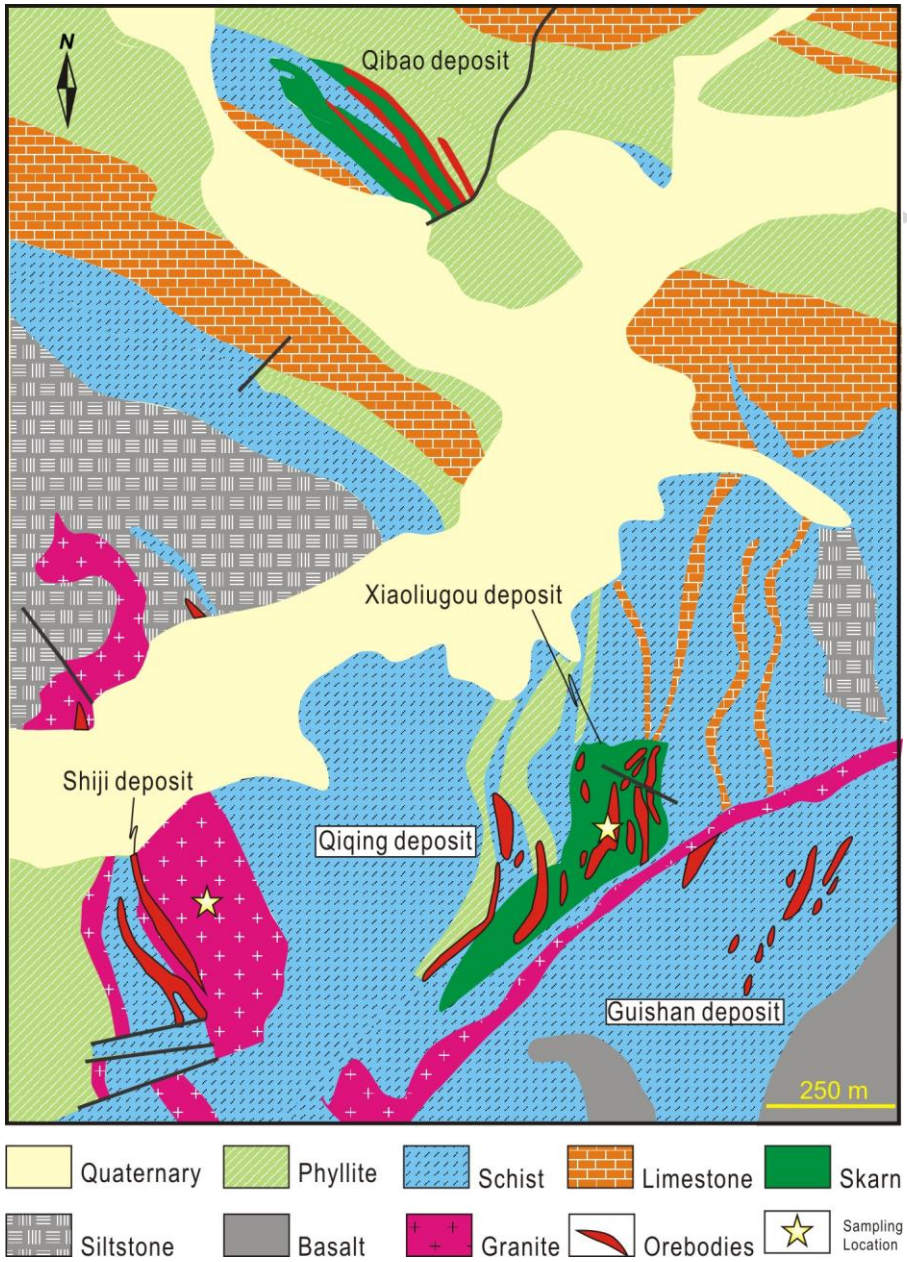

Figure 2

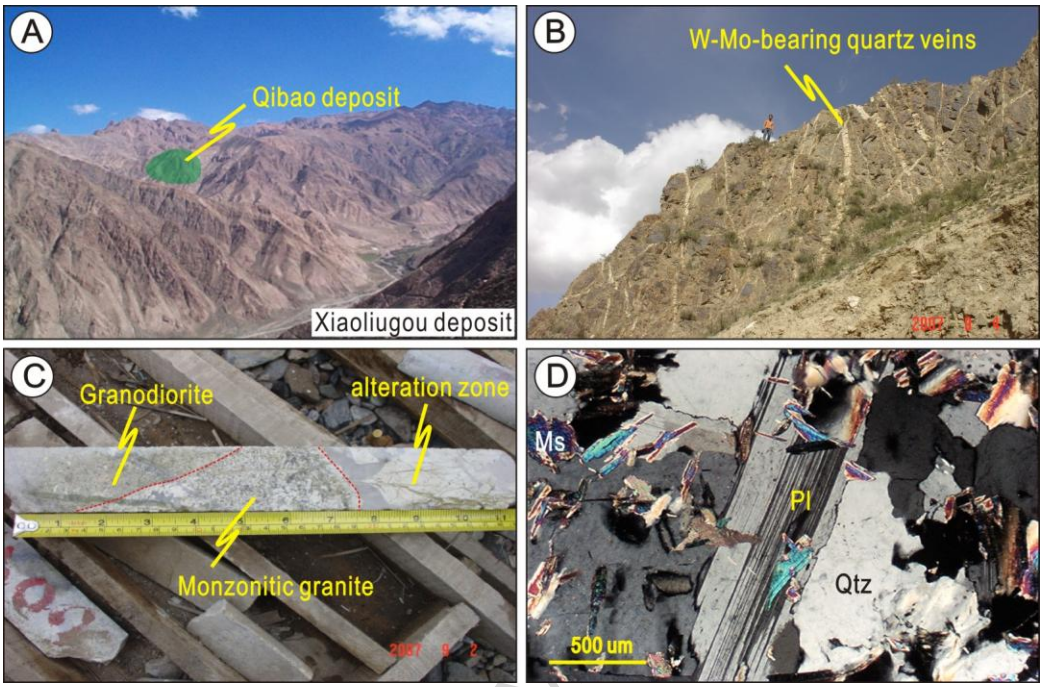

Figure 3

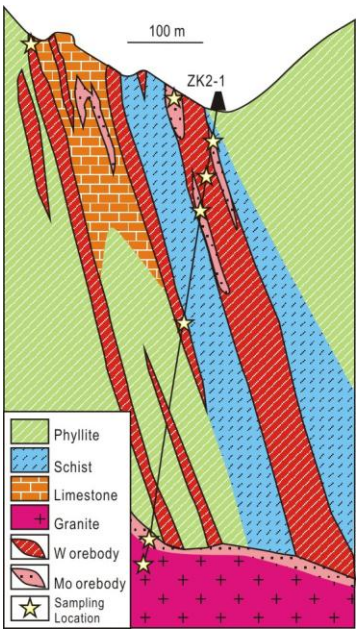

Figure 4

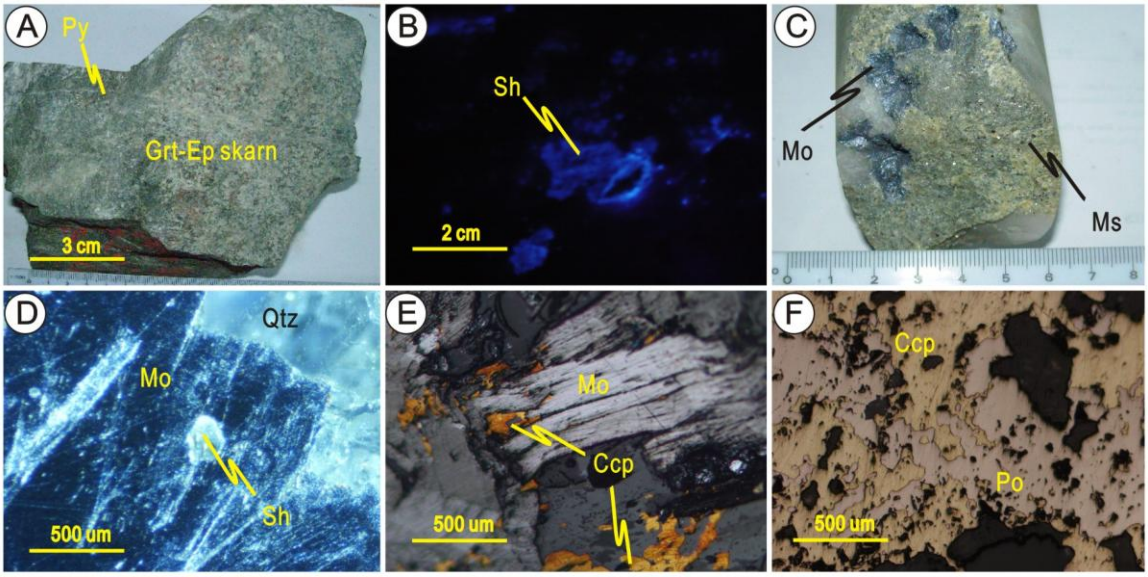

Figure 5

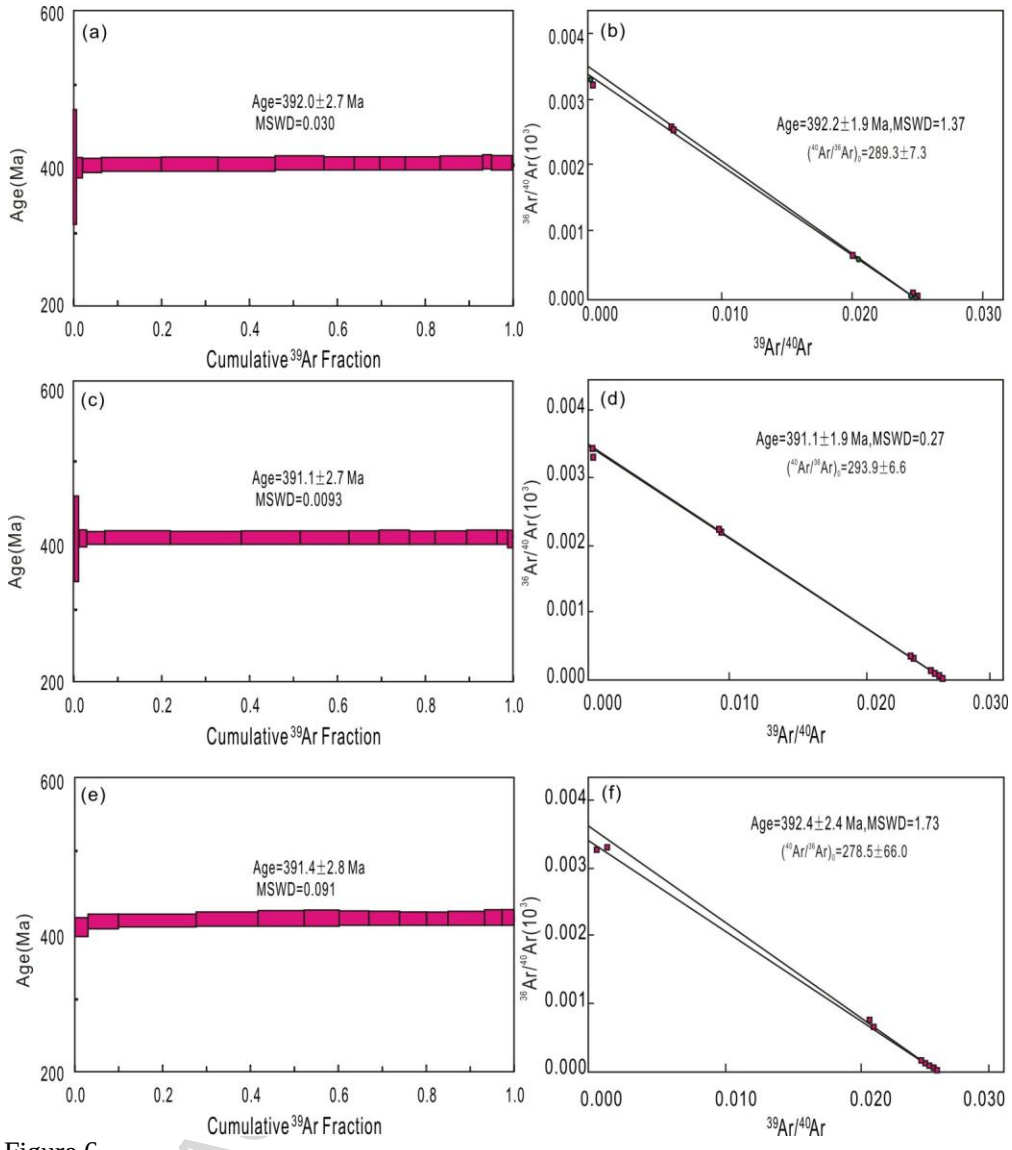

Figure 6

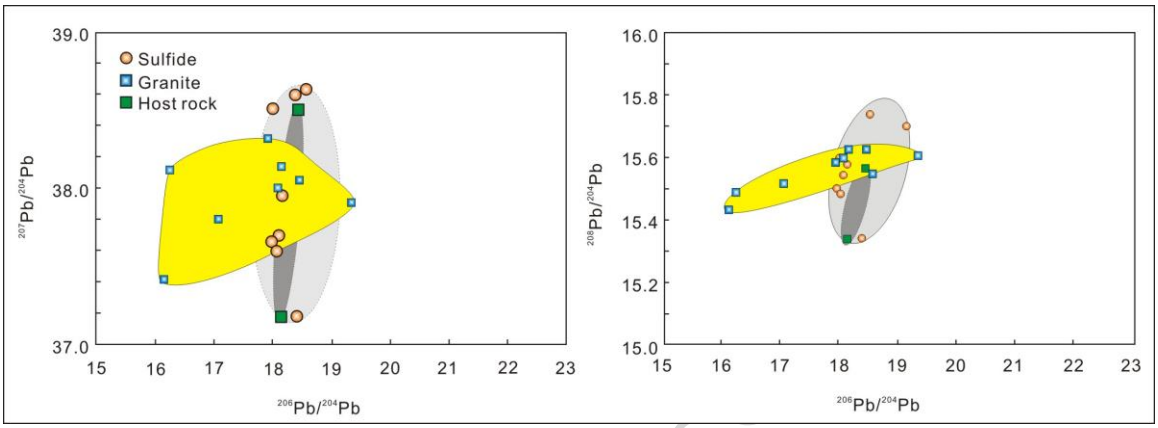

Figure 7

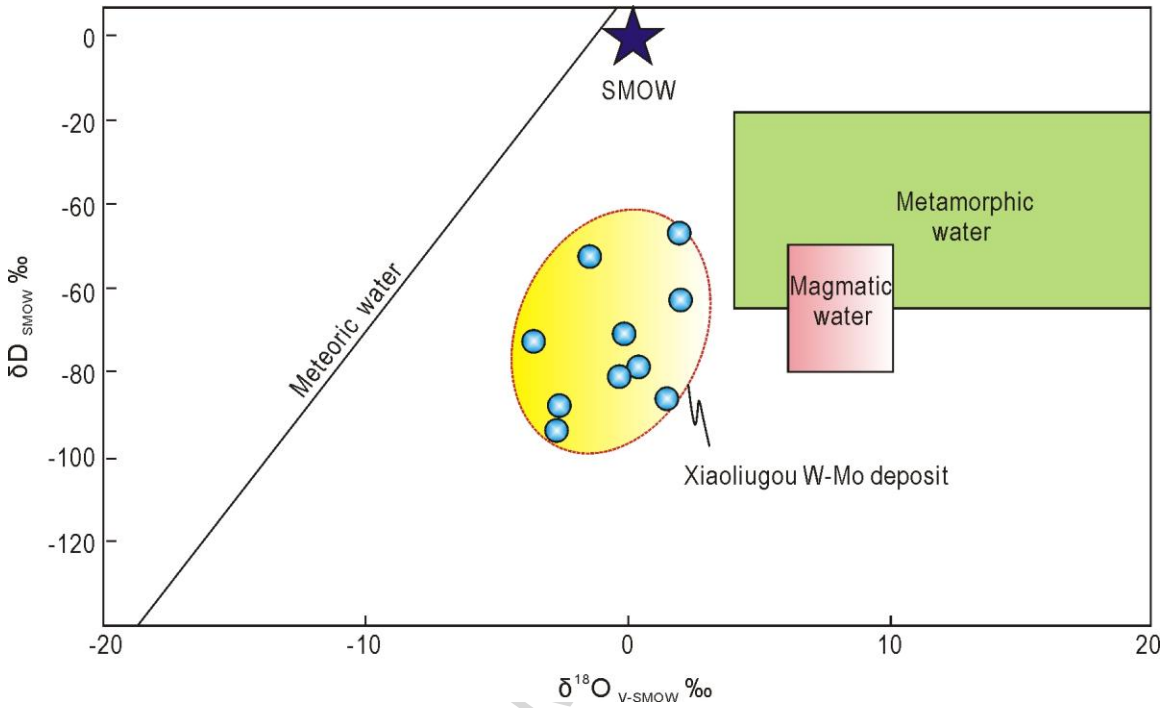

Figure 8

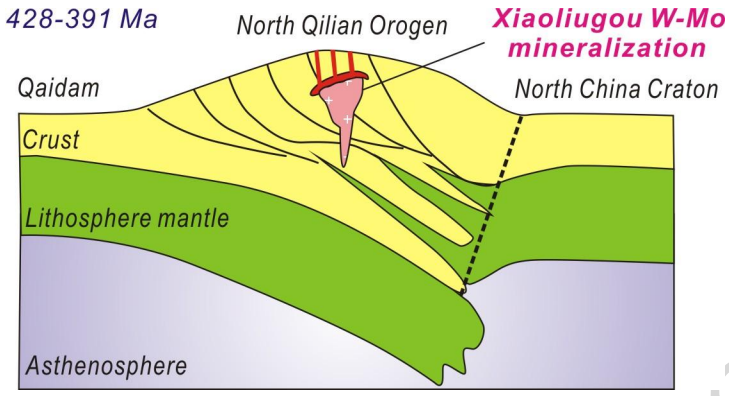

Figure 9

Table 1 Molybdenite Re-Os dating results

No.	Weight(g)	Re(10^{-6})	2σ	^{187}Re	2σ	^{187}Os	2σ	Model Age	2σ
*XL7-1	0.2555	2.266	0.024	1.419	0.015	10.17	0.5	436	12
*XL7-3	0.2113	4.972	0.044	3.112	0.027	23.67	0.82	462	17
*XL7-6	0.2001	8.74	0.268	5.471	0.168	42.74	0.16	475	15
*XL7-7	0.243	1.677	0.021	1.05	0.012	7.9	0.52	457	5
*XL7-10	0.2947	0.761	0.03	0.476	0.019	3.89	0.2	496	32
XLG-ZK-7	0.05067	6.216	0.049	3.907	0.031	27.92	0.23	427.4	6.0
ZKD-BK-7	0.05403	14.87	0.12	9.345	0.077	66.91	0.54	428.2	6.0

*Data source from Mao et al. (1999)

Table 2 Muscovite $^{39}Ar/^{40}Ar$ stepwise laser ablation dating results

T(℃)	$^{40}Ar/^{39}Ar$	$^{37}Ar/^{39}Ar$	$^{39}Ar/^{39}Ar$	$^{40}Ar^{*}/^{39}Ar_{K}$	$^{40}Ar^{*}$(%)	$^{39}Ar_{K}$(%)	Age(Ma)	2σ
PD30120-KZD-B2								
800	2370.23424	0.29547	7.75377	79.037818	3.33	0.03	715.8	431.8
860	1716.85834	0.03	5.28956	153.800117	8.96	0.35	1203	215.7
900	127.29594	0.0282	0.29905	38.930074	30.58	0.51	387.8	19.9
940	48.82182	0.00627	0.03387	38.813553	79.5	1.47	386.8	3.5
970	40.67679	0.00229	0.00511	39.16572	96.28	4.33	389.9	2.5
1000	39.62311	0.00051	0.00113	39.289171	99.16	13.56	391	2.3
1020	39.50454	0.00075	0.00067	39.306605	99.5	12.87	391.2	2.5
1040	39.51042	0.00067	0.00067	39.313113	99.5	13.02	391.2	2.3
1060	39.62336	0.00085	0.00062	39.439193	99.54	11.12	392.4	2.4
1080	39.77506	0.00106	0.00103	39.471071	99.24	6.87	392.6	2.3
1110	39.75698	0.00169	0.0012	39.403049	99.11	5.72	392	2.3
1140	39.87116	0.00231	0.00163	39.389227	98.79	5.78	391.9	2.3
1170	39.90933	0.00125	0.00148	39.47116	98.9	7.99	392.6	2.3
1200	39.82806	0.00076	0.00097	39.542551	99.28	9.7	393.3	2.3
1240	39.97985	0.00187	0.00122	39.617805	99.09	1.85	394	2.3
1450	40.58454	0.00471	0.00332	39.603192	97.58		393.8	2.5
PD30120-KZD-B5								
800	2168.82624	0.46073	7.16887	50.480909	2.33	0.03	486.9	440.3
860	1010.87866	0.18302	3.1398	83.096058	8.22	0.39	743.6	167.4
900	106.13985	0.01942	0.22603	39.35102	37.07	0.81	390.3	14.7
940	45.86197	0.00597	0.02198	39.365776	85.83	1.74	390.4	2.8
970	40.92231	0.0028	0.00534	39.345346	96.15	4.3	390.2	2.4
1000	39.72676	0.00089	0.0011	39.402762	99.18	14.84	390.7	2.4
1020	39.64798	0.00066	0.00059	39.472329	99.56	15.98	391.3	2.2
1040	39.58094	0.00081	0.00058	39.41023	99.57	13.46	390.8	2.3
1060	39.65526	0.00091	0.00062	39.47327	99.54	11.11	391.3	2.4
1080	39.74005	0.00108	0.00084	39.491656	99.37	6.86	391.5	2.3
1110	39.73054	0.00118	0.001	39.434573	99.25	6.93	391	2.5
1140	39.84691	0.00173	0.00116	39.504874	99.14	5.73	391.6	2.2
1170	39.779	0.00114	0.00119	39.428462	99.12	7.29	390.9	2.5
1200	39.96026	0.00114	0.00137	39.553962	98.98	6.77	392.1	2.3
1240	40.30613	0.00397	0.00253	39.557741	98.14	2.49	392.1	2.4
1450	41.6235	0.00545	0.00784	39.307129	94.43	1.26	389.9	3
PDQB-KZD-B4								
860	944.70127	2.60943	2.95765	71.080095	7.51	0.37	657.5	164.1
900	287.56536	1.45332	0.86134	33.195275	11.53	0.9	336.9	58
940	46.64735	0.02681	0.02936	37.973661	81.4	3.09	380.6	3.2
970	40.36719	0.00378	0.00528	38.806884	96.13	6.64	388.1	2.5
1000	39.4468	0.00147	0.00134	39.050522	99	17.56	390.3	2.3

1020	39.37127	0.00123	0.0007	39.16423	99.47	13.92	391.3	2.4
1040	39.48666	0.00143	0.00079	39.254173	99.41	10.41	392.1	2.6
1060	39.62955	0.00161	0.00107	39.313695	99.2	7.82	392.7	2.8
1080	39.68842	0.00206	0.00116	39.344652	99.13	6.7	392.9	2.3
1110	39.65168	0.00158	0.00125	39.280733	99.06	6.8	392.4	2.4
1140	39.72734	0.00194	0.00161	39.252493	98.8	5.96	392.1	2.4
1170	39.90037	0.00306	0.00217	39.260356	98.4	4.89	392.2	2.4
1200	40.09298	0.00258	0.00259	39.328008	98.09	8.22	392.8	2.5
1240	40.4942	0.00388	0.00339	39.492846	97.53	4.05	394.3	2.5
1450	40.90879	0.00645	0.00508	39.408966	96.33	2.69	393.5	2.7

Table 3 Sulfur isotopic compositions of pyrite and molybdenite

Sample	*Mineral*	*Occurrence*	$\delta^{34}S_{VCDT}$ ‰	$\delta^{34}S_{fuids}$ ‰
PD3223-B-21	Pyrite	Sulfide-bearing quartz	4.98	4.98
PDQB-ZD-B3	Pyrite	Sulfide-bearing quartz	13.17	13.17
XLG-ZK-7	Molybdenite	Sulfide-bearing quartz	11.03	11.03
ZPD-BK-7	Molybdenite	Sulfide-bearing quartz	11.67	11.67
*X17-1	Pyrite	Sulfide-bearing quartz	6.8	6.8
*X17-2	Molybdenite	Sulfide-bearing quartz	8.5	8.5
*X17-3	Pyrite	Sulfide-bearing quartz	8.8	8.8
*X17-6	Molybdenite	Sulfide-bearing quartz	8.1	8.1
*X17-1	Molybdenite	Sulfide-bearing quartz	7.7	7.7
*X17-6-1	Molybdenite	Sulfide-bearing quartz	8.2	8.2
*X18-1	Pyrite	Sulfide-bearing quartz	5.8	5.8
*X1-8	Pyrite	Sulfide-bearing quartz	9.9	9.9
*X17-10	Pyrite	Sulfide-bearing quartz	8.8	8.8
*X17-10	Molybdenite	Sulfide-bearing quartz	8.4	8.4

*Data from An and Zhou (2002)

Table 4 Lead isotopic data of sulfides, granite and ore-hosting sediments

No.	Sample	Pb	Th	U	$^{208}Pb/^{204}Pb$	$^{207}Pb/^{204}Pb$	$^{206}Pb/^{204}Pb$	$(^{208}Pb/^{204}Pb)i$	$(^{207}Pb/^{204}Pb)i$	$(^{206}Pb/^{204}Pb)i$
Sulfides										
XLG-ZK7	Molydbenite				38. 695	15.696	19.183			
ZPD-BK7	Molydbenite				38.117	15.73	21.73			
PD3223-B21	Pyrite				38.626	15.734	18.548			
PDQB-2D-B3	Pyrite				37.957	15.577	18.166			
*AT-1	Pyrite				37.687	15.542	18.099			
*AT-2	Pyrite				37.662	15.5	17.984			
*AT-3	Pyrite				37.6	15.481	18.04			
*AT-4	Chalcopyrite				38.592	18.809	18.382			
**JQZ-1	Pyrite				37.175	15.34	18.406			
**JQZ-2	Pyrite				38.501	15.597	18.02			
Average					**37.991**	**15.901**	**18.656**			
Host rocks										
*AT-5	Volcanics				37.175	15.34	18.152			
*AT-6	Volcanics				38.501	15.566	18.455			
Average					**37.838**	**15.453**	**18.304**			
Intrusion										
XLG-ZK10	Granite	42.8	11.3	17.5	38.424	15.723	20.266	38.051	15.624	18.472
XLG-ZK11	Granite	36.2	11.3	17.3	38.339	15.726	21.475	37.891	15.609	19.347
XLG-ZK12	Granite	46.3	12.5	23.4	38.239	15.673	20.798	37.856	15.550	18.572
XLG-ZK13	Granite	41.3	11.6	23.5	38.391	15.734	20.602	37.992	15.596	18.096
XLG-ZK14	Granite	14.7	14.2	27.4	38.868	15.919	24.887	37.407	15.436	16.143
XLG-ZK15	Granite	34.6	12.9	16.1	38.834	15.699	19.982	38.306	15.586	17.938
XLG-ZK16	Granite	29.9	13.8	8.1	38.787	15.693	19.345	38.140	15.628	18.170
XLG-ZK17	Granite	28.8	16.0	18.8	38.890	15.647	19.078	38.113	15.491	16.244
XLG-ZK18	Granite	26.7	16.3	16.7	38.657	15.670	19.806	37.797	15.519	17.072
Average		**33.48**	**13.32**	**18.75**	**38.603**	**15.720**	**20.693**	**37.950**	**15.560**	**17.784**

$^{208}Pb/^{204}Pb$, $^{207}Pb/^{204}Pb$, $^{206}Pb/^{204}Pb$ is the measured isotopic value at present, $(^{208}Pb/^{204}Pb)i$, $(^{207}Pb/^{204}Pb)i$, $(^{206}Pb/^{204}Pb)i$ is the corrected isotopic value based on the zircon crystallization age of 420 Ma.

*Data source from An and Zhou (2002)

**Data source from Mao et al. (1999)

Table 5 Quartz oxygen and hydrogen isotopic data

Sample	*Mineral*	δD_{SMOW}(‰)	$\delta^{18}O_{SMOW}$(‰)	$\delta^{18}O_{H2O}$(‰)	*Th(°C)*
XLG-I-1	Quartz	-86	12.4	1.75	217
XLG-I-3	Quartz	-79	12.9	0.67	192
XLG-ZK-2	Quartz	-73	9.5	-3.38	182
XLG-ZK-5	Quartz	-94	10.6	-2.42	180
XLG-ZK-8	Quartz	-71	11.7	0.13	202
XLG-ZK-13	Quartz	-89	9.8	-2.26	195
XLG-ZK-14	Quartz	-81	11.8	0.02	199
PD3223-B21	Quartz	-63	16.3	2.27	167
PDQB-ZD-B-3	Quartz	-47	15.2	2.34	183
XLG-ZK-7	Quartz	-53	11.4	-1.26	186

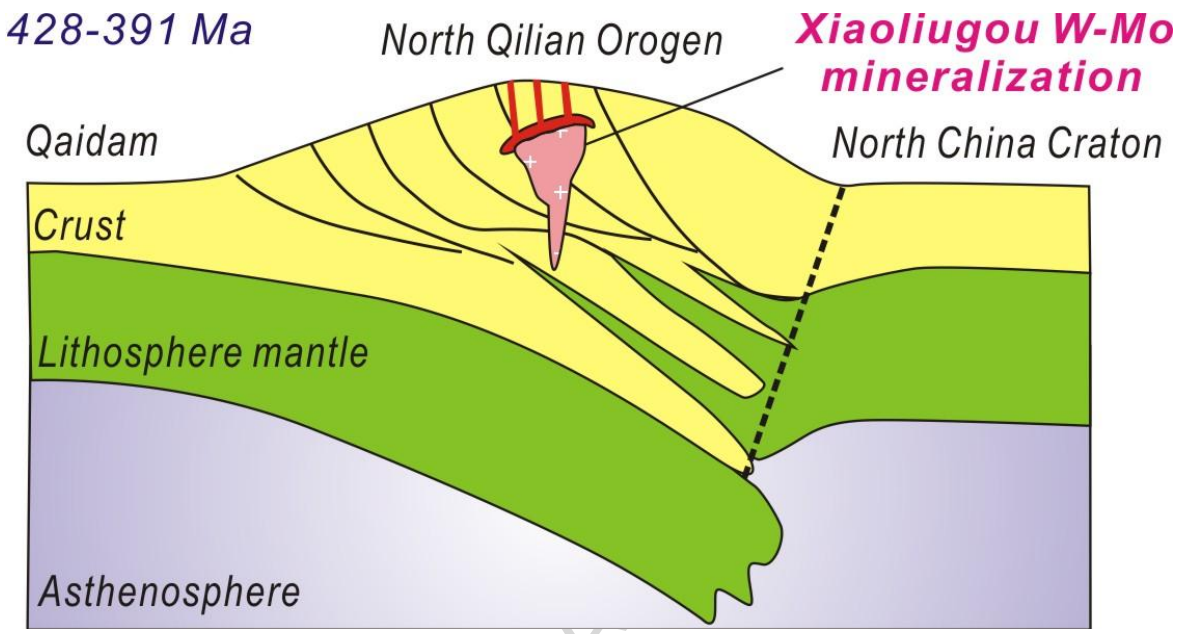

Graphical abstract

Highlights

1) A mineral sequence of scheelite > molybdenite > chalcopyrite was identified.
2) Re-Os and Ar-Ar dating constrained the mineralization to 428 – 391 Ma.
3) S-Pb-D-O geochemistry suggests metals and fluids sourced from granite and host rocks.
4) Xiaoliugou is a skarn system formed in a mid-Palozoic continental collision setting